THE BELL SYSTEM TECHNICAL JOURNAL

DEVOTED TO THE SCIENTIFIC AND ENGINEERING ASPECTS OF ELECTRICAL COMMUNICATION

Volume 61 October 1982 Number 8

The Tap-Leakage Algorithm: An Algorithm for the Stable Operation of a Digitally Implemented, Fractionally Spaced Adaptive Equalizer

By R. D. GITLIN, H. C. MEADORS, JR., and S. B. WEINSTEIN

(Manuscript received January 19, 1982)

A fractionally spaced equalizer is a nonrecursive adaptive filter whose tap weights are spaced a fraction of a symbol interval apart. Such an equalizer can significantly enhance modem performance in the presence of severe linear distortion, when compared with a conventional synchronous equalizer whose taps are spaced a symbol interval apart. However, a digitally implemented, fractionally spaced equalizer generally will exhibit long-term instability when the conventional tap-adjustment algorithm is used. This occurs because, in contrast to the synchronous equalizer, a fractionally spaced equalizer generally will have many sets of tap values, which result in nearly equal values of mean-squared error (mse). Some of these tap settings—which invariably will be attained because of biases in the digital tap-updating circuitry—are large enough to cause register overflows and consequent performance deterioration. In this paper we report how a simple modification in the tap-adjustment algorithm provides a solution to the above problem. The modified tap-adjustment algorithm prevents the buildup of large coefficient values by systematically "leaking" or decreasing the magnitudes of all the equalizer tap weights. For an experimental modem operating at 9.6 kb/s, it has been demonstrated that the tap-leakage adjustment algorithm prevents the accumulation of large equalizer tap values,

while permitting the full performance gain of a fractionally spaced equalizer to be realized.

I. INTRODUCTION

Fractionally spaced equalizers (FSEs), which are nonrecursive, tapped, delay-line adaptive filters, are currently receiving much attention[1-7] because of the significant performance advantage they provide when compared with a conventional synchronous equalizer. Since an FSE has the capability to adaptively realize the optimum linear receiver, it can greatly improve the performance of a modem in the presence of severe linear distortion. More specifically, significant performance improvements have been observed owing to the ability of an FSE to compensate effectively for delay distortion at the limits of private-line, voice-grade channel conditioning.[8] However, in laboratory experiments with a digitally implemented FSE it was noticed that after an extended period of operation some of the equalizer tap weights would invariably become large, while the mean-squared error (mse) remained at a satisfactory level. The taps generally would become so large that one or more registers, which compute partial sums of the equalizer output, would overflow, and the modem performance was then substantially degraded. This phenomenon is a consequence of the fact that an FSE, in contrast to a conventional synchronous equalizer, generally has many sets of tap values that correspond to roughly the same mse. Included in the set of tap values that correspond to the minimum mse are some tap coefficients of relatively large magnitude. These large tap values can be attained because of the cumulative effect of noise or any bias in the digital circuitry that performs the equalizer updating. Even though the value of the mse is satisfactory, some of these tap values will be large enough to cause occasional overflow of the partial sums computed to form the equalizer output. The purpose of this paper is twofold: to elucidate why a fractionally spaced equalizer has so many apparently "good" sets of tap values, and to indicate how equalizer operation can be stabilized by simply modifying the conventional estimated-gradient tap-adjustment algorithm.

The "almost unique" nature of the fractionally spaced equalizer coefficients is discussed in Section II. In Section III we describe the reasons for the occurrence of large tap values, and in Section IV a modified adjustment algorithm, dubbed the tap-leakage algorithm, is proposed to remedy the observed equalizer instability. The results of laboratory experiments are reported in Section V.

II. DOES A FRACTIONALLY SPACED EQUALIZER HAVE A UNIQUE OPTIMUM SETTING?

2.1 Fractionally spaced equalizers

To answer the question posed by the title of this section, we refer to the simplified baseband data transmission system shown in Fig. 1a.

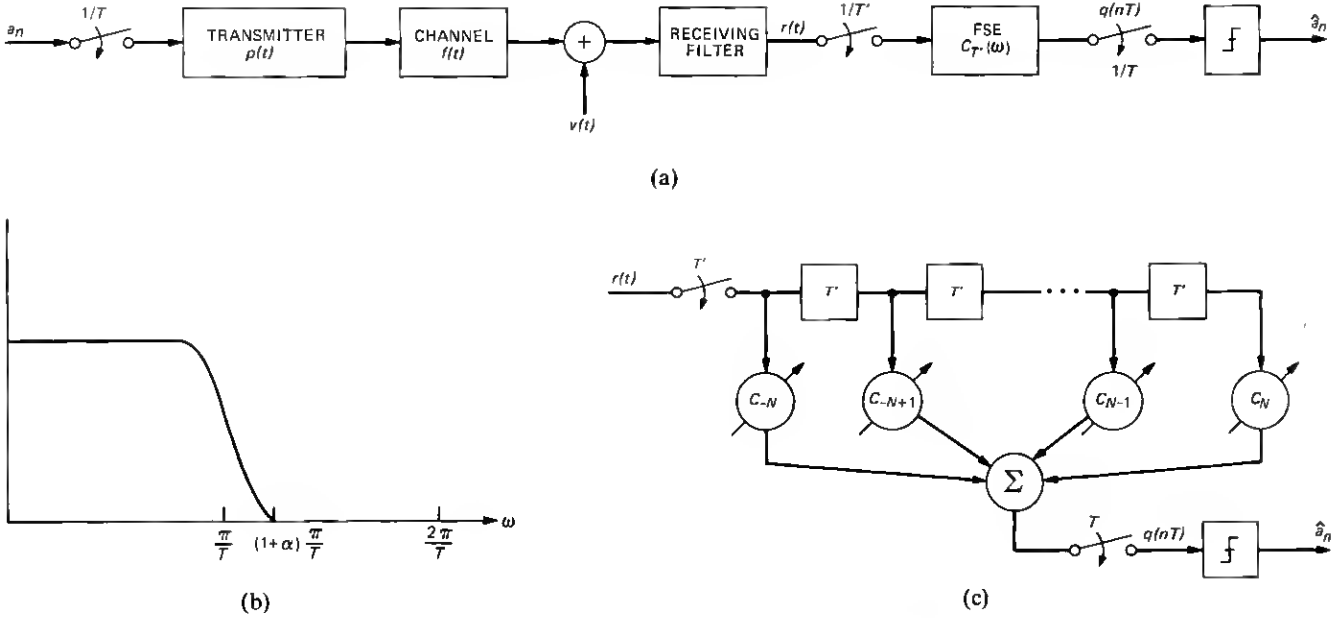

Fig. 1—Simplified (baseband) pulse amplitude modulation (PAM) data transmission system incorporating an FSE. (a) Transmission system. (b) Spectrum of the transmitted pulse. (c) A fractionally spaced equalizer.

For the purposes of exploring the phenomenon of large-tap buildup, this baseband model will suffice. Referring to the figure: $\{a_n\}$ are the discrete-valued multilevel data symbols, $1/T$ is the symbol rate, $p(t)$ is the band-limited transmitter pulse (whose spectrum is shown in Fig. 1b), $f(t)$ is the channel impulse response, and $v(t)$ is the additive background noise. Note that the receiving filter output, $r(t)$, is sampled at the rate $1/T'$, and the samples are then passed through the tapped delay-line equalizer (shown in Fig. 1c) having $(2N + 1)$ delay elements spaced $T'(<T)$ seconds apart and weighting coefficients $\{c_n\}$. The FSE output

$$q(nT) = \sum_{m=-N}^{N} c_m r(nT - mT'), \qquad n = 1, 2, \cdots \tag{1}$$

is computed at the symbol rate and quantized (sliced) to provide the data decision, $\hat{a}_n$. The transmitted pulse spectrum, shown in Fig. 1b, generally will be band-limited to $(1 + \alpha)\pi/T$ radians/second where the rolloff factor, α, varies between 0 and 1. An FSE with tap spacing T' seconds will have a transfer function, C_T, (ω), with period $2\pi/T'$, and, as shown in Fig. 2, if $T' < T/(1 + \alpha)$, the transfer function of the FSE will span the entire spectral range of the transmitted signal. This enables the equalizer to exert complete control over the amplitude and delay distortion present in the region $0 < |\omega| < (1 + \alpha)\pi/T$. Consequently, the FSE can compensate for these distortions directly, rather than filtering the aliased (folded) spectrum, as is done by the conventional equalizer.[9] As an example of this feature, consider the ability of the FSE to compensate for delay distortion by synthesizing the phase characteristic conjugate to that of the received pulse. This operation will leave the noise power at the equalizer output unchanged from the received noise power. The conventional synchronous equalizer, because it has a transfer function that has period $2\pi/T$, can only equalize the folded spectrum, i.e., the compensation characteristics on either

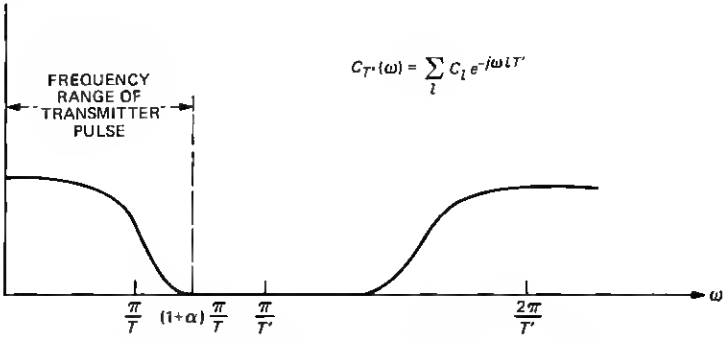

Fig. 2—Transfer function of a fractionally spaced equalizer.

side of π/T are restricted to be the conjugate of one another. If the channel characteristics are such that the folded spectrum has a relative null at a particular frequency, then the noise at the output of the synchronous equalizer can be significantly enhanced and the performance degraded proportionately.

From Fig. 2 it should also be evident that when the noise becomes vanishingly small, there is legitimate concern as to what function(s) the equalizer will synthesize in the region, $(1 + \alpha)\pi/T < |\omega| < 2\pi/T$, where there is no signal energy. It is known[7,8] that for an infinitely long equalizer the transfer characteristic that minimizes the mse is

$$C_T, (\omega) = \frac{X^*(\omega)}{\sum_l \left| X\left[\omega + l\frac{2\pi}{T}\right]\right|^2 + N_0}, \qquad |\omega| \leq \frac{2\pi}{T}, \tag{2}$$

where the asterisk denotes the complex conjugate, $X(\omega)$ is the transfer function of the received pulse,† $x(t)$, presented to the equalizer input, and N_0 is the noise spectral density. As long as $N_0 \neq 0$, the equalizer function is zero whenever the received signal has no power; however, as $N_0 \to 0$ the derivation of (2) is no longer valid, and, moreover, (2) approaches 0/0 in the region $(1 + \alpha)\pi/T < |\omega| < \pi/T$. Clearly, as the noise vanishes, an infinitely long FSE can synthesize the required channel characteristic in the region $0 < |\omega| < (1 + \alpha)\pi/T$, and an arbitrary—and nonunique—characteristic in the remaining frequency band. An interesting question, then, is what happens to the optimum tap setting for a finite length FSE as the noise becomes vanishingly small.

2.2 *Uniqueness of solution for finite length FSE as the noise vanishes*

The equalized mse is defined as

$$E = \langle [q(nT) - a_n]^2 \rangle = \langle e_n^2 \rangle, \tag{3}$$

where the brackets denote the ensemble average with respect to the data symbols and the noise, and e_n is the equalizer output error, $q(nT) - a_n$, at $t = nT$. The mse is readily evaluated as the quadratic form

$$E = \mathbf{c}'A\mathbf{c} - 2\mathbf{c}'\mathbf{x} + \langle a_n^2 \rangle, \tag{4}$$

where the prime denotes the transposed vector, $\mathbf{c}'$ is the tap vector $(c_{-N}, \cdots, c_0, \cdots, c_N)$, $\mathbf{x}'$ is the truncated impulse-response vector $|x(NT'), \cdots, x(-NT')|$, and A is the channel-correlation matrix. More specifically, the channel vector is given by

$$\mathbf{x} = \langle a_n \mathbf{r}_n \rangle, \tag{5}$$

† Thus $x(t)$ is the convolution of the transmitter, channel, and receiver filters.

where the received vector is given by $\mathbf{r}_n' = [r(nT + NT'), \cdots, r(nT), r(nT - NT')]$, and the A matrix is defined by

$$A = \langle \mathbf{r}_n \mathbf{r}_n' \rangle. \tag{6}$$

The klth element of the channel correlation matrix is given by

$$A_{kl} = \sum_{m=-\infty}^{\infty} x(mT - kT')x(mT - lT') + \sigma^2 \delta_{k-l}, \tag{7}$$

where σ^2 is the noise variance and δ_k is the Kronecker delta. Note that A is not a Toeplitz matrix, as it would be for a synchronous equalizer ($T' = T$). If A is nonsingular then the optimum setting and the corresponding minimum mse are obtained from (4) by differentiation, and are given by

$$\mathbf{c}_{\text{opt}} = A^{-1}\mathbf{x} \tag{8a}$$

$$E_{\text{opt}} = 1 - \mathbf{x}'A^{-1}\mathbf{x}, \tag{8b}$$

where $\langle a_n^2 \rangle$ is taken to be unity.

As seen from (7), the matrix A is the sum of two matrices, and as will be evident from the discussion that follows, the channel-dependent component of A is always positive semidefinite. Since the other component of the channel-correlation matrix, $\sigma^2 I$, is positive definite, then A will also be positive definite, and we can conclude that when there is noise present, the optimum tap setting is unique.

We now consider the situation as the noise becomes vanishingly small; clearly, the optimum tap setting will be unique if, and only if, A is nonsingular. A sufficient condition for A to be nonsingular is the nonvanishing of the quatratic form $\mathbf{u}'A\mathbf{u}$, for any *nonzero* test vector $\mathbf{u}$ with components $[u_i]$. Let us consider in detail this quadratic form, which we write from (7) as:

$$\begin{aligned}
\mathbf{u}'A\mathbf{u} &= \sum_{m,n=-N}^{N} u_m A_{mn} u_n \\
&= \sum_{m,n=-N}^{N} u_m u_n \sum_{l=-\infty}^{\infty} x(lT - nT')x(lT - mT') \\
&= \sum_{l=-\infty}^{\infty} \left[\sum_{m=-N}^{N} u_m x(lT - mT') \right]^2 \geq 0.
\end{aligned} \tag{9}$$

The above inequality establishes the positive semidefinite nature of the matrix A, and we see from (9) that $\mathbf{u}'A\mathbf{u}$ can vanish only if*

* The authors gratefully acknowledge discussions with J. E. Mazo that led to this development.

$$\sum_{m=-N}^{N} u_m x(lT - mT') = 0 \qquad l = 0, \pm 1, \pm 2, \cdots . \tag{10}$$

If we define the periodic Fourier transform

$$U_{T'}(\omega) = \sum_{m=-N}^{N} u_m e^{j\omega mT'}, \qquad |\omega| \le \frac{\pi}{T'}, \tag{11}$$

then we can proceed further by noting that

$$\begin{aligned}
\sum_{m=-N}^{N} u_m x(lT - mT') &= \sum_{m=-N}^{N} u_m \int_{-\infty}^{\infty} X(\omega) e^{j\omega(lT - mT')} \frac{d\omega}{2\pi} \\
&= \int_{-\infty}^{\infty} \left[\sum_{m=-N}^{N} u_m e^{-j\omega mT'} \right] X(\omega) e^{-j\omega lT} \frac{d\omega}{2\pi} \\
&= \int_{-\infty}^{\infty} U_{T'}(\omega) X(\omega) e^{-j\omega lT} \frac{d\omega}{2\pi} \\
&= \sum_{k} \int_{(2k-1)\frac{\pi}{T}}^{(2k+1)\frac{\pi}{T}} U_{T'}(\omega) X(\omega) e^{-j\omega lT} \frac{d\omega}{2\pi} \\
&= \int_{-\frac{\pi}{T}}^{\frac{\pi}{T}} \left[\sum_{k} U_{T'} \left(\omega + \frac{k2\pi}{T} \right) \right. \\
&\qquad \left. \cdot X \left(\omega + \frac{k2\pi}{T} \right) \right] e^{-j\omega lT} \frac{d\omega}{2\pi}.
\end{aligned} \tag{12}$$

The right-hand side of (12) is recognized as the sample, at $t = lT$, of a function whose Fourier transform, $Z_{eq}(\omega)$, is contained in the brackets. If (12) is to be zero for every value of l, then it must be that the Fourier transform inside the integral vanishes completely, i.e.,

$$Z_{eq}(\omega) \equiv \sum_{k} U_{T'} \left(\omega + \frac{k2\pi}{T} \right) X \left(\omega + \frac{k2\pi}{T} \right) = 0, \qquad |\omega| \le \frac{\pi}{T}. \tag{13}$$

In Fig. 3a we show the situation when there is no excess bandwidth, and since the sum, (13), reduces to one term, the only way for $Z_{eq}(\omega) \equiv 0$ is for either $X(\omega) \equiv 0$ or $U_{T'}(\omega) \equiv 0$. Since this implies that $U_{T'}(\omega) \equiv 0$, it would violate the nonzero requirement on $\mathbf{u}$. Thus, we can conclude for this case that A is positive definite. A similar sketch for the less than 100-percent excess bandwidth case is shown in Fig. 3b, where it is noted that only the $k = 0, \pm 1$ terms contribute to the sum, (13). However, in the nonrolloff region, $|\omega| \le (1 - \alpha)\pi/T$, only the $k = 0$ term influences the sum. For channels that do not vanish over the entire nonrolloff region, it is clear that for $Z_{eq}(\omega)$ to vanish it

CONDITIONS FOR WHICH $Z_{eq}(\omega) = \sum_k U_{T'}\left(\omega + \frac{k2\pi}{T}\right) X\left(\omega + \frac{k2\pi}{T}\right) = 0, |\omega| \leq \frac{\pi}{T}$

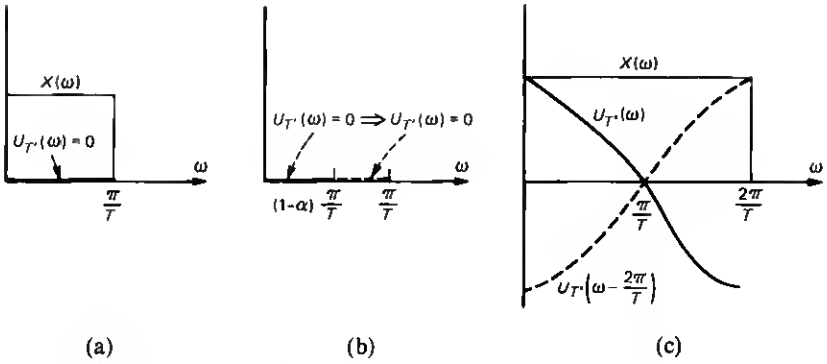

Fig. 3—Sketches associated with eq. (13). (a) $\alpha = 0$. (b) $0 < \alpha < 1$. (c) $\alpha = 1$.

is required that $U_T(\omega)$ vanish at least over the entire nonrolloff region. Since $U_{T'}(\omega)$ is a finite-term Fourier series, it cannot vanish over an interval without vanishing everywhere, which in turn would again make $\mathbf{u} = 0$. Note that if the channel vanished over a portion of the nonrolloff region, then since $Z_{eq}(\omega)$ is a finite-term Fourier series, its energy could not be totally concentrated in the region where there was no channel energy. Thus, the solution still would be unique. It is worth noting that in the extreme case of 100-percent excess bandwidth, $Z_{eq}(\omega)$ can vanish. For example, in Fig. 3c we sketch the situation for a constant $X(\omega)$, and with $U_{T'}(\omega) = \cos \omega T/2$ it is apparent that $Z_{eq}(\omega) \equiv 0$. Thus, for a finite-length FSE with an excess bandwidth of less than 100 percent, we can conclude that even as the noise becomes vanishingly small, the A matrix is nonsingular and there is a unique optimum tap setting.

We digress for a moment to point out that for a finite-length synchronous equalizer where $T' = T$, (13) indicates that since $U_T(\omega + k2\pi/T) = U_T(\omega)$, we can conclude that if the folded channel spectrum does not vanish completely, then there is always a unique tap setting.

III. THE TAP-WANDERING PHENOMENON

3.1 Motivation, background, and infinite-precision considerations

We have shown that for a finite-length fractionally spaced equalizer and the practical range of interest—where the excess bandwidth is on the order of 10 to 50 percent—even with vanishingly small noise there will always be a unique best tap setting. One issue of interest is the

"closeness" (or ill-conditioning) of the A matrix to a singular matrix. This is important for two reasons. First, the distribution of the eigenvalues of A, which is a measure of the ill-conditioning of the matrix, influences the rate of convergence of the equalizer taps to their optimum setting.[10] Second, and more importantly, we observe, from (4) that the contours of equal mse are elliptical, and the eccentricity of these contours is directly related to the eigenvalue distribution. In the appendix it is shown that for an infinitely long equalizer with $T' = T/2$, half the eigenvalues are zero; in Fig. 4 we illustrate some constant mse contours for a finite-length $T/2$ equalizer, whose optimum tap setting is denoted by $\mathbf{c}_{opt}$. Recall[10] that even with an infinite-precision analog implementation, the use of a finite step-size in the conventional estimated-gradient tap-adjustment algorithm results in a steady-state mse that exceeds* E_{opt}. This is depicted in Fig. 4, where the boldface contour is the mse that can be attained with the chosen step-size. Owing to the random component in the algorithm's correction term, the taps will wander along the constant mse contour, and there will be a certain probability that the taps will become so large that one or more registers will saturate.† Thus, even in an analog implementation, random tap wandering can, in principle, lead to degraded performance.

3.2 A model for tap drifting in digital equalizer

It has been observed in laboratory experiments with a digitally implemented FSE, that under control of the conventional estimated-gradient tap adjustment algorithm,[10]

$$\mathbf{c}_{n+1} = \mathbf{c}_n - \alpha[\mathbf{e}_n\mathbf{r}_n], \qquad n = 1, 2, 3, \cdots \tag{14}$$

the equalizer taps inevitably drift close to the shaded (large tap) region of Fig. 4. In (14), $\mathbf{c}_n$ is the tap vector at $t = nT$, α is a positive value called the step-size, which influences both the convergence rate of the equalizer and the steady-state mse, and the brackets around $\mathbf{e}_n\mathbf{r}_n$ indicate that this increment is quantized to a specified number of bits. The term $[\mathbf{e}_n\mathbf{r}_n]$ will have a deterministic component proportional to the desired gradient, and a random component owing to both the manner in which the digital quantization is performed and the influence of the noise and data-dependent terms. Generally, $[\mathbf{e}_n\mathbf{r}_n]$ will also possess a deterministic component owing to bias inevitably present in a digital implementation. A typical mechanism for such a bias is the two's complement type of quantizing characteristic shown in Fig. 5. To quantify our discussion, we denote the bias by a time-invariant

---

* The mse E_{opt} is achieved when the taps are at their optimum values, $\mathbf{c}_{opt}$.

† For a synchronous equalizer the ellipses will not be very eccentric, and the tap wandering will not do any damage.

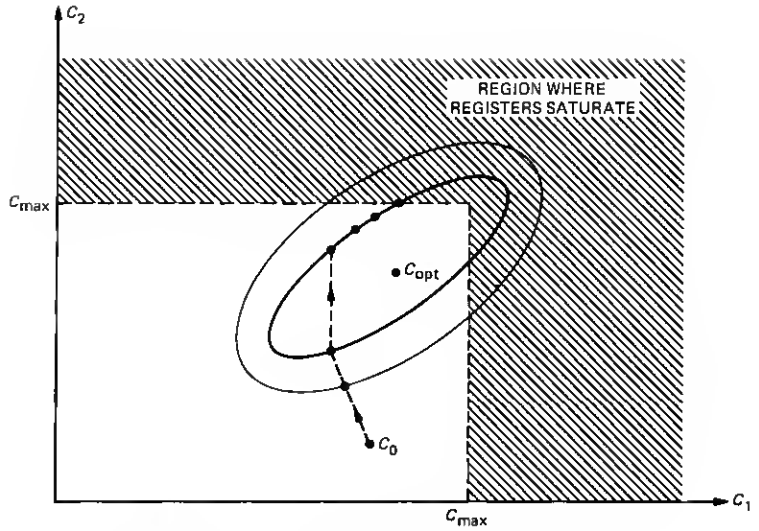

Fig. 4—Contours of equal mse and tap convergence.

vector, $\mathbf{b}$, and model the adjustment algorithm as

$$\mathbf{c}_{n+1} = \mathbf{c}_n - \alpha(\mathbf{e}_n\mathbf{r}_n + \mathbf{b}), \tag{15}$$

where the bias vector has equal components, and b has a magnitude of less than half a quantization interval. Equation (15) ignores, except for the bias, the effect of limited precision on the algorithm.* Since it has been observed in the laboratory that tap wandering results in a systematic buildup of some tap values, the model expressed by (15) should be useful in relating the magnitude of the bias to the other system parameters. It is bias component that can drive, in a *deterministic* manner,† the tap vector towards the tap region corresponding to large tap values. Since the equalizer output is formed as a series of partial sums, of the form $\sum_m c_m r_{n-m}$, it is clear that large-tap values can lead either to an overflow of a partial sum or saturation of a tap. As the taps grow, occasional register overflows begin to occur, resulting in noise-like "hits" on the equalizer output. The occurrence of such a "hit" is a function of the specific pattern of data samples contained in the equalizer. Continued growth of the taps increases the frequency of the "hits" as more data patterns can produce these events. The error rate can become very high, relative to what constitutes acceptable performance, but the frequency of occurrence of "hits" is still low

* Reference 10 discusses the effect of limited precision on the mse or an RSE in the absence of a bias term. Note that the bias as "seen" by the taps is αb.

† As opposed to the random wandering associated with the self-noise of the algorithm.

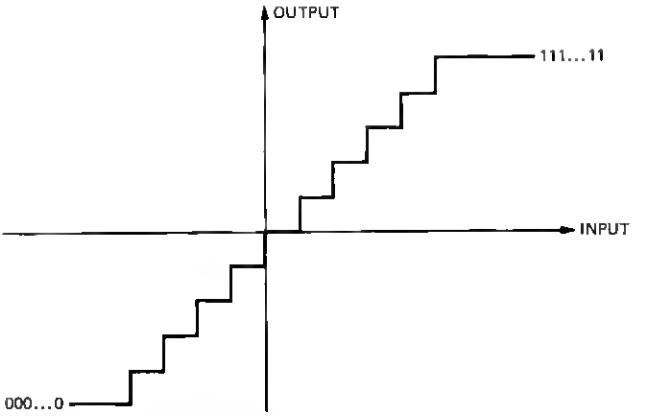

Fig. 5—Quantizing characteristic that produces a bias in the tap-adjustment algorithm.

enough that the mse is almost unaffected. Growth continues until the tap coefficients themselves begin to saturate. At this point severe degradation occurs as the degrees of freedom of the system are reduced. In fact, with an experimental digitally implemented FSE, with a symbol rate of 2400 symbols/second, overflows typically begin to occur within several minutes of operation. The overflows produce noise-like hits and a degraded equalizer output.

3.3 The mean tap error and the mean-squared error

To assess the effects of the bias quantitatively we first define the tap-error vector,

$$\boldsymbol{\epsilon}_n \equiv \mathbf{c}_n - \mathbf{c}_{\text{opt}}, \tag{16}$$

and then use the model described by (15) to write the tap-error evolution as

$$\boldsymbol{\epsilon}_{n+1} = \boldsymbol{\epsilon}_n - \alpha(\mathbf{e}_n\mathbf{r}_n + \mathbf{b}). \tag{17}$$

The mse at the nth iteration,* E_n, is given by

$$E_n = E_{\text{opt}} + \langle \boldsymbol{\epsilon}_n' A \boldsymbol{\epsilon}_n \rangle. \tag{18}$$

Our intent is to study the excess mse,

$$q_n \equiv \langle \boldsymbol{\epsilon}_n' A \boldsymbol{\epsilon}_n \rangle, \tag{19}$$

and the mean tap error vector, $\langle \boldsymbol{\epsilon}_n \rangle$, in the presence of the bias, $\mathbf{b}$.

* In arriving at (18), we assume that iterations are infrequent enough so that successive vectors $\{\mathbf{r}_n\}$ are independent. In practice, adjustments are generally made at the symbol rate, and the algorithm is observed to behave as if the $\{\mathbf{r}_n\}$ were independent. This phenomenon is discussed in Ref. 11.

From (17) we have

$$\langle \epsilon_{n+1} \rangle = \langle \epsilon_n \rangle - \alpha \langle e_n \mathbf{r}_n \rangle - \alpha \mathbf{b} = (I - \alpha A)\langle \epsilon_n \rangle - \alpha \mathbf{b}, \tag{20}$$

and thus the steady-state mean tap error satisfies

$$\langle \epsilon \rangle = A^{-1}\mathbf{b}. \tag{21}$$

If λ_i and $\mathbf{p}_i$, respectively, denote the ith eigenvalue and eigenvector of A, then

$$\langle \epsilon \rangle = \sum_{-N}^{N} \frac{\mathbf{p}_i'\mathbf{b}}{\lambda_i} \mathbf{p}_i . \tag{22}$$

Clearly, if there is a small eigenvalue whose eigenvector is *not* orthogonal to $\mathbf{b}$, then the steady-state tap error can be quite large. It is interesting to note that for a small number of taps, one would expect that the eigenvalues not be small, i.e., the equalizer would not possess enough degrees of freedom to realize a somewhat arbitrary transfer function beyond the rolloff region. Consider the one-tap equalizer (or automatic gain control) where $A = \langle r^2(nT) \rangle$, and consequently

$$\langle \epsilon \rangle = \frac{\mathbf{b}}{\langle r^2(nT) \rangle}. \tag{23}$$

Thus, for a one-tap equalizer, the tap error is directly proportional to the magnitude of the bias, and the buildup of a large tap value is prohibited. However, in the limit as the number of taps becomes infinite, it is shown in the appendix that with $T' = T/2$, half the eigenvalues are zero, while the other half tend to uniformly sample the aliased (with respect to the symbol rate) squared magnitude of the channel transfer function. Moreover, the eigenvectors corresponding to the zero eigenvalues have most of their energy concentrated near $1/T$ Hz (and are thus close to being orthogonal to $\mathbf{b}$), while the ith eigenvector corresponding to the nonzero eigenvalues approaches a sinusoid of radian frequency $\omega_i = i/N\ \pi/T$. For practical, finite-length equalizers, these limiting conditions will only be approximated, and there will be small eigenvalues whose corresponding eigenvector is not orthogonal to $\mathbf{b}$. Consequently, $\langle \epsilon \rangle$ can become as large as the largest ratio $[\mathbf{p}_i'\mathbf{b}]/\lambda_i$, and the steady-state tap error would then be biased away from the optimum value.

We now discuss the effect of the bias term on the equalized mse,

$$E_n = E_{\text{opt}} + \langle \epsilon_n' A \epsilon_n \rangle , \tag{24}$$

where the tap error evolves according to (17). In particular we will examine the size of the residual mse,

$$q_n \equiv \langle \epsilon_n' A \epsilon_n \rangle . \tag{25}$$

An exact analysis (or tight bounds) of the behavior of q_n is an extremely difficult problem; however, by assuming that the sequence $\{\mathbf{r}_n\}$ is independent,[11] and that when the taps are at or near their optimum settings, the squared output error is relatively insensitive to the transmitted data pattern,* it is possible to establish simple, but useful, relationships between the relevant system parameters. From (17) we have that

$$q_{n+1} = \langle \boldsymbol{\epsilon}'_{n+1} A \boldsymbol{\epsilon}_{n+1} \rangle = \langle [\boldsymbol{\epsilon}'_n - \alpha(e_n \mathbf{r}'_n + \mathbf{b}')] A [\boldsymbol{\epsilon}_n - \alpha(e_n \mathbf{r}_n + \mathbf{b})] \rangle, \quad (26)$$

and by using the above assumptions we have (see Ref. 10)

$$q_{N+1} \cong [1 - 2\alpha\bar{\lambda} + \alpha^2 \lambda_M (2N+1)\langle r_n^2 \rangle] q_n + \alpha^2 \lambda_M (2N+1)(\langle r_n^2 \rangle E_{\text{opt}} + b^2), \quad (27)$$

where λ_M is the maximum eigenvalue of A, and where

$$\bar{\lambda} = \frac{1}{2N+1} \sum_{-N}^{N} \lambda_i \quad (28)$$

is the average eigenvalue. Thus, the steady-state fluctuation about the minimum mse is

$$q_\infty \cong \frac{\alpha \lambda_M (2N+1)[\langle r^2(nT) \rangle E_{\text{opt}} + b^2]}{2\bar{\lambda} - \alpha \lambda_M (2N+1)\langle r^2(nT) \rangle}. \quad (29)$$

To assess the effect of the bias on q_∞, we note that the bias "seen" by a tap component, αb, will be approximately $2^{-B} C_{\max}$, where B is the number of bits used to represent the tap weights and $C_{\max}$ is the maximum tap value. If the equalized signal is assumed to have unity power, then $C_{\max} \approx 1/[(2N+1)\langle r_n^2 \rangle]^{1/2}$ and α is typically[10] on the order of $1/|(2N+1)\cdot\langle r_n^2 \rangle|$. Thus, $b^2/|r^2(nT)|$ will be on the order of $2^{-2B}(2N+1)$, and when the equalized output signal power is unity, E_{opt} is roughly the inverse of the output signal-to-noise ratio. With typical parameters like $(2N+1) = 60$, $B = 12$, and $E_{\text{opt}} = 0.001$, it is clear that the effect of the bias on q_∞ is negligible. Thus, owing to the quantizing bias, there can be, on the average, a buildup of one or more large-tap weights, while the mse is relatively unaffected. In other words, under the influence of a bias the taps would still remain on the boldface mse contour of Fig. 4, but would spend most of the time near the shaded region, and the system would be subject to random overflows, or hits. This phenomenon has been repeatedly observed experimentally, and in the next section we will describe a very simple means of controlling the tap wandering.

* When the taps are at their optimum values, the error is known to be uncorrelated with the received samples.

IV. THE TAP-LEAKAGE EQUALIZER ADJUSTMENT ALGORITHM

As we have discussed in the previous section, some or all of the tap weights in an FSE can reach unacceptably large values when the conventional tap adjustment algorithm, (14), is used. A simple means of controlling large-tap buildup is by minimizing either of the augmented cost functions

$$J_1 = E + \mu \sum_{i=-N}^{N} c_i^2, \tag{30a}$$

$$J_2 = E + \mu \sum_{i=-N}^{N} |c_i|, \tag{30b}$$

where, as in (3), E is the mse and μ is a suitably chosen (small) constant. The cost function J_1 ascribes a quadratic penalty to the magnitude of the tap vector, while J_2 provides a magnitude penalty, i.e., the cost function is penalized whenever the tap vector builds up excessively. Since the taps are to be adjusted adaptively, we cannot interpret μ as a Lagrange multiplier. The use of a Lagrange multiplier would be appropriate if we were actually able to minimize J in a deterministic manner by using the true gradient. However, since the gradient of E with respect to $\mathbf{c}$, $A\mathbf{c} - \mathbf{x}$, is not available, we must implement a stochastic algorithm analogous to (14). Thus, μ must be chosen beforehand by using some prior knowledge of the system parameters.

4.1 Increased steady-state mse: true-gradient algorithm

As a preliminary calculation, let us first consider the degradation in the minimum attainable steady-state mse caused by choosing $\mathbf{c}$ to minimize J_1 instead of E. Note that, for the moment, we are neglecting the bias and only assessing the increased mse caused by minimizing tbe augmented cost function, J_1, via the true-gradient algorithm. From (4) we observe, for binary transmission, that the taps will attempt to minimize the modified criterion:

$$J_1 = \mathbf{c}'(A + \mu I)\mathbf{c} - 2\mathbf{c}'\mathbf{x} + 1. \tag{31}$$

$$= \mathbf{c}'B\mathbf{c} - 2\mathbf{c}'\mathbf{x} + 1, \tag{32}$$

where $B = A + \mu I$. The matrix B has the same eigenvectors as A, while the eigenvalues of B are $\lambda + \mu$. Note that the contours of equal values of J_1 are still ellipses but tbe maximum-to-minimum eigenvalue ratio governing the tap wandering is now $(\lambda_{max} + \mu)/(\lambda_{min} + \mu)$, where λ_{max} and λ_{min} are the maximum and minimum eigenvalues of A, respectively. Thus, by choosing μ properly, the eccentricity can be controlled, and the equalizer tap vector is now determined as if the noise power were increased from σ^2 to $\sigma^2 + \mu$. Of course, the use of a

tap vector selected on the basis of the pseudo-noise power, $\sigma^2 + \mu$, will increase the steady-state mse.* Note that the steady-state tap vector will now satisfy

$$B\mathbf{c} = \mathbf{x}$$

or

$$\mathbf{c}(\mu) = B^{-1}\mathbf{x} = (A + \mu I)^{-1}\mathbf{x}, \tag{33}$$

where $\mathbf{c}(\mu)$ denotes the steady-state tap vector corresponding to the chosen value of μ. Thus, the minimum attainable mse is given by

$$E(\mu) = \mathbf{c}'(\mu)A\mathbf{c}(\mu) - 2\mathbf{c}'(\mu)\mathbf{x} + 1, \tag{34}$$

and the increased mse, $E(\mu) - E_{\text{opt}}$, is

$$E(\mu) - E_{\text{opt}} = [\mathbf{c}(\mu) - \mathbf{c}_{\text{opt}}]'A[\mathbf{c}(\mu) - \mathbf{c}_{\text{opt}}]. \tag{35}$$

To make a more detailed evaluation of the increase in mse, we let

$$\epsilon(\mu) = \mathbf{c}(\mu) - \mathbf{c}_{\text{opt}} \tag{36}$$

denote the tap-error vector. Recalling the diagonalization

$$A = \sum_{i=-N}^{N} \lambda_i \mathbf{p}_i \mathbf{p}_i', \tag{37}$$

and the fact that inverse matrices have the same eigenvectors and inverse eigenvalues, we find that

$$\begin{aligned}\epsilon(\mu) = \mathbf{c}(\mu) - \mathbf{c}_{\text{opt}} &= [(A + \mu I)^{-1} - A^{-1}]\mathbf{x} \\ &= \sum_i \left(\frac{1}{\lambda_i + \mu} - \frac{1}{\lambda_i}\right) \mathbf{p}_i \mathbf{p}_i' \mathbf{x} \\ &= -\sum_i \frac{\mu}{\lambda_i(\lambda_i + \mu)} \mathbf{p}_i' \mathbf{x} \cdot \mathbf{p}_i.\end{aligned} \tag{38}$$

Substituting (38) into (35), and using the orthogonality property of distinct eigenvectors, we find that

$$E(\mu) - E_{\text{opt}} = \mu^2 \sum_{i=-N}^{N} (\mathbf{p}_i'\mathbf{x})^2 \frac{1}{\lambda_i(\lambda_i + \mu)^2}. \tag{39}$$

Thus, to a first approximation, the increased mse grows only as the square of the leakage parameter, μ, while the eigenvalue distribution—and the range in which the taps can wander—can be favorably altered, in a significant manner, by using even a very small value of μ.

* The fluctuation about the minimum mse, caused by the finite step size, will also be examined.

4.2 The adaptive tap-leakage algorithm

In a manner analogous to the commonly used estimated gradient algorithm, the adaptive tap-leakage algorithms are constructed, from (30a), by minimizing the augmented instantaneous squared error, $e_n^2 + \mu \mathbf{c}_n' \mathbf{c}_n$, and, from (30b), by minimizing $e_n^2 + \mu \sum_{i=-N}^{N} |c_n^{(i)}|$. The first algorithm modifies the gradient by a term proportional to the tap vector itself, giving the algorithm

$$\begin{aligned} \mathbf{c}_{n+1} &= \mathbf{c}_n - \alpha[e_n \mathbf{r}_n + \mu \mathbf{c}_n] \\ &= (1 - \alpha\mu)\mathbf{c}_n - \alpha e_n \mathbf{r}_n, \end{aligned} \tag{40a}$$

while the second algorithm is of the form

$$\begin{aligned} \mathbf{c}_{n+1} &= \mathbf{c}_n - \alpha(e_n \mathbf{r}_n + \mu \operatorname{sgn} \mathbf{c}_n) \\ &= \mathbf{c}_n - \alpha\mu \operatorname{sgn} \mathbf{c}_n - \alpha e_n \mathbf{r}_n, \end{aligned} \tag{40b}$$

where the sgn operation is applied individually to each component of the tap vector. Note that from an implementation point of view, the algorithm can be modified with almost no hardware change other than applying a systematic decrement to the magnitude of each tap. The second algorithm (40b) has the practical advantage that adjustments will continue to be made no matter how small any tap weight becomes, while the first algorithm has the "advantage" of analytical tractability.

Consider now the mean tap error when the leakage algorithm (40a) is used. In the presence of digital bias, the algorithm is modeled as

$$\mathbf{c}_{n+1} = \mathbf{c}_n - \alpha[e_n \mathbf{r}_n + \mathbf{b} + \mu \mathbf{c}_n]. \tag{41}$$

Subtracting $\mathbf{c}_{\text{opt}}$ from both sides of (41), and solving for the steady-state average tap error we find

$$\begin{aligned} \langle \boldsymbol{\epsilon} \rangle &= (A + \mu I)^{-1}\mathbf{b} + (A + \mu I)^{-1}\mu A^{-1}\mathbf{x} \\ &= \sum_{i=-N}^{N} \frac{\mathbf{p}_i'\mathbf{b}}{\lambda_i + \mu}\mathbf{p}_i + \mu \sum_{i=-N}^{N} \frac{\mathbf{p}_i'\mathbf{x}}{\lambda_i(\lambda_i + \mu)}\mathbf{p}_i. \end{aligned} \tag{42}$$

The first term, on the right-hand side of (42), is similar to (22), but note that the eigenvalues have been modified to eliminate the catastrophic effects that can accompany vanishingly small eigenvalues. The second term, which is proportional to the leakage parameter, is similar to (39), and represents the increased tap error caused by the minimization of J_1 and not E. The leakage parameter, μ, must be chosen sufficiently large so that the first term is properly controlled in magnitude, but not so large that the magnitude of the second term becomes appreciable. In general, the choice of μ is best done empirically, but if μ is chosen to be in the range where $\lambda_{\text{minimum}} + \mu \approx \mu$, then equating the magnitude of the two terms in (42) gives

$$\mu \approx \frac{\sum_{i=-N}^{N} (\mathbf{p}_i'\mathbf{b})^2}{\sum_{i=-N}^{N} \frac{(\mathbf{p}_i'\mathbf{x})^2}{\lambda_i^2}}. \tag{43}$$

For any given channel, (43) can be evaluated, but as far as the average tap error is concerned, it is sufficient to choose μ in such a way that the magnitude of $\langle \epsilon \rangle$ is within the nonshaded region of Fig. 4. From (42), one reasonable choice is to make μ roughly equal to the smallest value of λ_i for which $\mathbf{p}_i'\mathbf{x}$ is significantly larger than λ_i.

To assess the effect of the tap-leakage algorithm, (40a), on the steady-state mse we recall eq. (18)

$$E_n = E_{\text{opt}} + q_n,$$

where E_{opt} is the minimum mse when both $\mathbf{b}$ and μ are zero. From (41) we can compute an approximation to the steady-state value, q_∞, in a manner similar to the computation of (28). For the adaptive tap-leakage algorithm we find that the fluctuation about the minimum mse is

$$q_\infty \approx \frac{\alpha\lambda_M[(2N+1)\cdot\langle r^2(nT)\rangle E_{\text{opt}} + \mathbf{b}'\mathbf{b}] + 2\alpha\mu\mathbf{b}'\mathbf{x} + \mu^2\mathbf{x}'A^{-1}\mathbf{x}}{2\bar{\lambda} + \mu(1-\alpha\bar{\lambda}) - \alpha[\lambda_M(2N+1)\langle r^2(nT)\rangle + \mu^2]}. \tag{44}$$

Obviously, (44) is very channel dependent, but when μ is chosen on the order of a small eigenvalue, then the fluctuation about the minimum mse is a rather insensitive function of the leakage parameter, while the magnitude of the mean tap error, (42), can be effectively controlled by the proper choice of μ.

In the next section we will discuss the results of laboratory experiments that use the tap-leakage algorithm to control the potentially unstable operation of a fractionally spaced equalizer.

V. LABORATORY EXPERIMENTS

For an experimental 9.6-kb/s data transmission system using 16-point quadrature amplitude modulation, the tendency of the tap coefficients of a digitally implemented equalizer with $T/2$ sample spacing to drift is demonstrated by the waveforms of Figs. 6a and 6b. These waveforms are analog representations of the values of one component of a set of complex tap coefficients associated with data samples taken $T(=1/2400)$ second apart. The equalizer is physically constructed by using two conventional T-spaced interleaved structures, requiring four tap coefficient component distributions to totally describe the state of the equalizer.

The equalizer goes through a conventional start-up procedure, except that timing recovery and carrier phase adjustments are suppressed

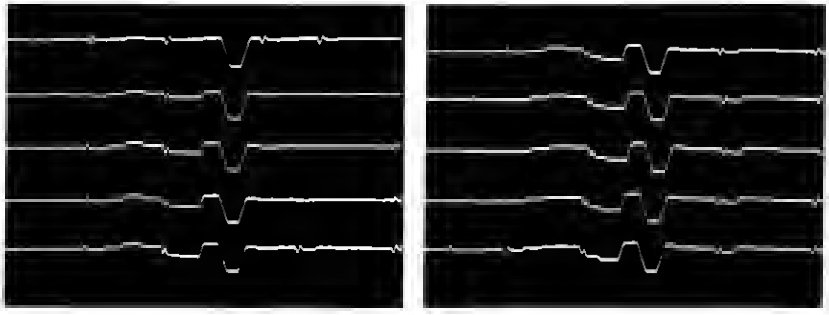

(a) (b)

Fig. 6—Tap buildup as a function of time. (a) Three-minute intervals. (b) Five-minute intervals.

so that the distribution of tap coefficients will not change through interaction with either of these operations. The transmitted signal is fed back to the receiver, after passing through appropriate attenuators, thus avoiding any time varying channel characteristics, and assuring a low noise environment.

The first trace of Fig. 6a illustrates the distribution of components among the particular collection of coefficients immediately after start-up. A single large negative component is noted, with all other components relatively insignificant. The coefficients are updated in the usual fashion, via (14), without the addition of a tap-leakage adjustment. Subsequent traces in Fig. 6a are taken at 3-minute intervals. The traces of Fig. 6b are a continuation of Fig. 6a with the separation in time extended to five minutes. A clear pattern of buildup in the amplitude of the taps, particularly those immediately preceding the original dominant tap, is demonstrated. A similar compensatory buildup occurs among those tap coefficient components not displayed, such that the mse is essentially unchanged over the duration of the test. This deterministic growth of tap amplitudes will eventually lead to saturation of shift register accumulators used in forming the various components of the equalizer passband outputs. The observed output signal constellation will display frequent apparent noise-like hits of large amplitude, and an unacceptable output error rate results.

The tap-coefficient components in the laboratory configuration are stored in 24-bit shift registers. The 12 most significant bits are used in the multiplication to form tap-product outputs. The remaining bits were to average out the effects of tap updating, which is normally done according to the rule

$$\mathbf{c}_{n+1} = \mathbf{c}_n - \alpha(e_n\mathbf{r}_n).$$

The components of the updating quantity $-\alpha(e_n\mathbf{r}_n)$ are stored in 12-bit

words which are added to the 20 most significant bits of the coefficients during the normal steady-state mode of operation. To counteract bias in the arithmetic, the updating is changed to the tap-leakage algorithm

$$\mathbf{c}_{n+1} = \mathbf{c}_n - \beta \operatorname{sgn} \mathbf{c}_n - \alpha(\mathrm{e}_n \mathbf{r}_n), \tag{45}$$

where $\beta = \alpha\mu$ of (40b). In the experimental setup, a count of 1 is added or subtracted to the 23rd most significant bit of each component of each tap coefficient once each symbol interval. In steady-state operation, the 12-bit updating signal will typically show activity in a minimum of the five least significant bits. In general, therefore, the leakage term is quite small compared with the conventional updating term.

The effect of introducing this leakage is shown in the waveforms of Fig. 7. The top trace shows the coefficient distribution 40 minutes after initial start-up, at the time the leakage is enabled. Subsequent traces were taken at 30-second intervals. Within two minutes the coefficient components had been virtually restored to the state that existed immediately after start-up.

The experimental arrangement allows the leakage to be scaled over a wide range. Viewing the 24-bit coefficient as an integer, the leakage increment can be made 2^r, $r = 0, 1, \cdots, 7$ ($r = 1$ is the case displayed). Since the coefficients are chosen to span an analog range of ± 4, this corresponds to β as defined in (45) ranging from 2^{-21} to 2^{-14}, with $\beta = 2^{-20}$ displayed. The value of α used in the experiment is $\alpha = 2^{-11}$. It is observed that $\beta = 2^{-21}$, the lowest possible level of continuous leakage, is adequate to suppress tap drift, indicating the extreme low level of the system bias to which the FSE updating algorithm appears susceptible.

The larger the value of β that is chosen, the more the leakage will degrade the equalizer performance, although the degradation is negligible for β less than 2^{-17}. In normal data-set operation, it is observed

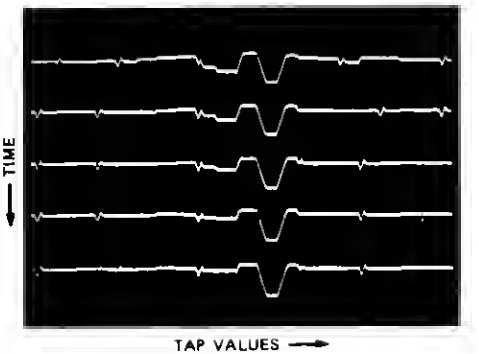

Fig. 7—The effect of the tap-leakage algorithm (30-second intervals between traces).

that a substantially rapid shift in the sampling epoch, which may occur during the timing recovery operation, will greatly accelerate the buildup of tap coefficients. The choice of $\beta = 2^{-18}$ will allow rapid response to this situation without perceivable performance degradation.

VI. CONCLUSIONS

Effective control of tap drifting for a fractionally spaced equalizer, at a 9.6-kb/s data rate, has been demonstrated by employing the easily implemented tap-leakage algorithm. The tap-leakage algorithm, or some variation of it, might be appropriate for any digitally implemented adaptive system that has too many degrees of freedom and that exhibits coefficient wandering.

APPENDIX

Asymptotic Distribution of the Eigenvalues and Eigenvectors for Synchronous and Fractionally Spaced Equalizers

In this appendix we describe the eigenvalues and eigenvectors of infinitely long synchronous and fractionally spaced equalizers.

A.1 Synchronous equalizer

First we recall the eigenvalues and eigenvectors of an infinitely long synchronous equalizer. From (7) we have the eigenvalue equation

$$\sum_{l=-N}^{N} A_{k-l} p_l = \lambda p_k, \qquad N \le k \le N, \tag{46}$$

where λ is an eigenvalue and $\mathbf{p}' = (p_{-N}, \cdots, p_0, \cdots, p_N)$ is the associated eigenvector. As $N \to \infty$, taking the Fourier Transform of both sides of (46) yields

$$A(\omega)P(\omega) = \lambda P(\omega), \qquad |\omega| \le \frac{\pi}{T}, \tag{47}$$

where

$$A(\omega) = \left| \sum_k X\left(\omega + \frac{k2\pi}{T}\right) \right|^2 + \sigma^2$$

$$= |X_{\text{eq}}(\omega)|^2 + \sigma^2, \qquad |\omega| < \frac{\pi}{T}. \tag{48}*$$

The only way for (47) to be satisfied [with $P(\omega) \not\equiv 0$] is for $P(\omega)$ to be concentrated at a single frequency [unless $A(\omega)$ has the same value at

* Recall that the Nyquist-equivalent spectrum $X_{\text{eq}}(\omega)$ is defined as $X_{\text{eq}}(\omega) = \sum_k X(\omega + k2\pi/T)$.

more than one frequency]. If we let

$$\omega_i = \frac{i}{N}\frac{\pi}{T},$$

then the solution to (47) is

$$\lambda_i = A(\omega_i)$$

$$-N \le i \le N$$

$$P_i(\omega) = \delta(\omega - \omega_i). \tag{49}$$

Thus, for a synchronous equalizer the asymptotic ($N \to \infty$) eigenvalues uniformly sample the folded-channel plus noise spectrum, and the eigenvectors are the corresponding sinusoids.

A.2 Fractionally Spaced Equalizer

Here the channel-correlation matrix, while symmetric, is not Toeplitz; thus Fourier Transform techniques do not yield the eigenvalues and eigenvectors in the above short order. For convenience we consider the noiseless situation, and the eigenvalue equation becomes

$$\sum_{l=-N}^{n} A(kT', lT')p(lT') = \lambda p(kT') \qquad -N < k < N, \tag{50}$$

where the channel-correlation matrix has elements

$$A(kT', lT') = \sum_m x(mT - kT')x(mT - lT'). \tag{51}$$

With $T' = T/2$ and $N \to \infty$ we write (50) for even and odd values of k

$$\sum_{l\,\text{even}} A\left(k\frac{T}{2}, l\frac{T}{2}\right) p\left(l\frac{T}{2}\right) + \sum_{l\,\text{odd}} A\left(k\frac{T}{2}, l\frac{T}{2}\right) p\left(l\frac{T}{2}\right) = \lambda p\left(k\frac{T}{2}\right), \; k \text{ even} \tag{52}$$

$$\sum_{l\,\text{even}} A\left(k\frac{T}{2}, l\frac{T}{2}\right) p\left(l\frac{T}{2}\right) + \sum_{l\,\text{odd}} A\left(k\frac{T}{2}, l\frac{T}{2}\right) p\left(l\frac{T}{2}\right) = \lambda p\left(k\frac{T}{2}\right), \; k \text{ odd}. \tag{53}$$

Now (52) and (53) can be written respectively as

$$\sum_l A(kT, lT)p(lT) + \sum_l A\,(kT, lT) + \frac{T}{2}\,p\left(lT + \frac{T}{2}\right) = \lambda p(kT), \qquad -\infty < k < \infty \tag{54}$$

and

$$\sum_l A\left(kT+\frac{T}{2}, lT\right)p(lT)+\sum_l A\left(kT+\frac{T}{2}, lT+\frac{T}{2}\right)p\left(l\frac{T}{2}\right)$$
$$=\lambda p\left(kT+\frac{T}{2}\right), \quad (55)$$

where both equations hold for all integer values of k, and, more importantly, the various component matrices are now all Toeplitz.* If we let

$$\tilde{X}_{eq}(\omega) \triangleq X(\omega)-X\left(\omega-\frac{2\pi}{T}\right)-X\left(\omega+\frac{2\pi}{T}\right), \qquad |\omega| \le \frac{\pi}{T} \quad (56)$$

and

$$\tilde{P}(\omega) \triangleq P(\omega)-P\left(\omega\frac{2\pi}{T}\right)-P\left(\omega+\frac{2\pi}{T}\right), \qquad |\omega| \le \frac{\pi}{T}, \quad (57)$$

then taking the synchronous Fourier Transform (i.e., with respect to the T seconds sampling interval) of (54) and (55) gives

$$|X_{eq}(\omega)|^2P(\omega)+X_{eq}(\omega)\tilde{X}^*_{eq}(\omega)\tilde{P}(\omega)=\lambda P(\omega) \qquad 0 \le |\omega| \le \frac{\pi}{T} \quad (58)$$

and

$$\tilde{X}_{eq}(\omega)X^*_{eq}(\omega)P(\omega)+|\tilde{X}_{eq}(\omega)|^2\tilde{P}(\omega)=\lambda\tilde{P}(\omega). \quad (59)$$

Note that $p(kT+T/2)$ has the Fourier Transform

$$e^{-j\omega\frac{T}{2}}\tilde{P}(\omega),$$

while the Transform of $p(kT)$ is of course $P(\omega)$. Arguing as we did for the synchronous equalizer, we see that the ith eigenvectors $P_i(\omega)$ and $\tilde{P}_i(\omega)$ must again be delta functions at $\omega_i = i/N\,\pi/T$. Upon setting the determinant of the pair (58) and (59) to zero, we see that the eigenvalues satisfy

$$\lambda_i^2-\lambda_i||X_{eq}(\omega_i)|^2+|\tilde{X}_{eq}(\omega_i)|^2|=0, \quad (60)$$

and thus for each value of ω_i there are two eigenvalues

$$\lambda_i = 0$$

$$\lambda_i = |X_{eq}(\omega_i)|^2+|X_{eq}(\omega_i)|^2=\sum_k\left|X\left(\omega_i+\frac{k2\pi}{T}\right)\right|^2. \quad (61)$$

In contrast to the synchronous equalizer, half of the eigenvalues are

* For example, $A(kT, lT+T/2)=\sum_m x(mT-kT)x(mT-lT+T/2)=\sum_n x(nT)x|nT+(k-l)T+T/2|$.

exactly zero, while the other half are samples of the aliased magnitude-squared channel transfer function. Not surprisingly, the eigenvalues are independent of the receiver sampling phase. Once the eigenvalues are determined we can solve for the eigenvectors. The ith eigenvector associated with the *zero* eigenvalue is

$$p_i\left(n\frac{T}{2}\right) = \begin{cases} \tilde{X}^*_{\text{eq}}(\omega_i)e^{j\omega_i nT}, & n \text{ even} \\ -X^*_{\text{eq}}(\omega_i)e^{j\omega_i\left(n+\frac{1}{2}\right)T}, & n \text{ odd,} \end{cases} \tag{62}$$

while the eigenvector associated with the *nonzero* eigenvalue is

$$p_i\left(n\frac{T}{2}\right) = \begin{cases} X_{\text{eq}}(\omega_i)e^{j\omega_i nT}, & n \text{ even} \\ \tilde{X}_{\text{eq}}(\omega_i)e^{j\omega_i\left(n+\frac{1}{2}\right)T}, & n \text{ odd.} \end{cases} \tag{63}$$

At this point we remark that when ω_i is not in the rolloff region then $X_{\text{eq}}(\omega_i) = \tilde{X}_{\text{eq}}(\omega_i)$, and (63) describes a sinusoid of frequency ω_i, since the even and odd portions of $p_i(n\ T/2)$ mesh together in a continuous manner [i.e.,

$$p_i(n\ T/2) = X_{\text{eq}}(\omega_i)e^{j\omega_i n\ T/2}].$$

However, (62) describes a function that changes sign and oscillates almost a full cycle in T seconds. Consequently, $p_i(n\ T/2)$, as given by (62), will have most of its spectral energy concentrated near $1/T$ Hz. When ω_i is in the rolloff region, the frequency content of (62) and (63) will differ somewhat from the above extreme cases but the general results will still be as above.

REFERENCES

1. A. Gersho, private communication, 1969.
2. D. M. Brady, "An Adaptive Coherent Diversity Receiver for Data Transmission Through Dispersive Media," Conference Record ICC 1970, pp. 21–35 to 21–40.
3. D. M. Brady, "Adaptive Signal Processor for Diversity Radio Receivers," U. S. Patent No. 3,633,107, filed June 4, 1970, issued January 4, 1972.
4. L. Guidoux, "Equaliseur Autoadaptif à Double Echantillonnage," L'Onde Electrique, *55* (January 1975), pp. 9–13.
5. O. Macchi and L. Guidoux, "A New Equalizer: the Double Sampling Equalizer," Ann. Telecommun. *30* (1975), pp. 331–8.
6. G. Ungerboeck, "Fractional Tap-Spacing Equalizers and Consequences for Clock Recovery for Data Modems," IEEE Trans. on Commun., *COM-24*, No. 8 (August 1976), pp. 856–64.
7. S. U. H. Qureshi and G. D. Forney, Jr., "Performance and Properties of a $T/2$ Equalizer," Conference Record NTC 1977 (December 1977).
8. R. D. Gitlin and S. B. Weinstein, "Fractionally-Spaced Equalization: An Improved Digital Transversal Equalizer," B.S.T.J., *60*, No. 2 (February 1981), pp. 275–96.
9. R. W. Lucky, J. Salz, and E. J. Weldon, Jr., *Principles of Data Communication*, New York: McGraw-Hill, 1968.
10. R. D. Gitlin and S. B. Weinstein, "On the Required Tap Weight Precision for Digitally-Implemented Adaptive Equalizers," B.S.T.J., *58*, No. 2 (February 1979), pp. 301–21.
11. J. E. Mazo, "On The Independence Theory of Equalizer Convergence," B.S.T.J., *58*, No. 5 (May–June 1979), pp. 963–93.